

## Enhancing energy harvesting potential of (K,Na,Li)NbO<sub>3</sub>-epoxy composites via Li substitution

Deutz, Daniella B.; Mascarenhas, Neola T.; van der Zwaag, Sybrand; Groen, Wilhelm A.

**DOI**

[10.1111/jace.14698](https://doi.org/10.1111/jace.14698)

**Publication date**

2016

**Document Version**

Accepted author manuscript

**Published in**

Journal of the American Ceramic Society

**Citation (APA)**

Deutz, D. B., Mascarenhas, N. T., van der Zwaag, S., & Groen, W. A. (2016). Enhancing energy harvesting potential of (K,Na,Li)NbO<sub>3</sub>-epoxy composites via Li substitution. *Journal of the American Ceramic Society*, 100(3), 1108–1117. Advance online publication. <https://doi.org/10.1111/jace.14698>

**Important note**

To cite this publication, please use the final published version (if applicable). Please check the document version above.

**Copyright**

Other than for strictly personal use, it is not permitted to download, forward or distribute the text or part of it, without the consent of the author(s) and/or copyright holder(s), unless the work is under an open content license such as Creative Commons.

**Takedown policy**

Please contact us and provide details if you believe this document breaches copyrights. We will remove access to the work immediately and investigate your claim.

# Enhancing energy harvesting potential of (K,Na,Li)NbO<sub>3</sub>-epoxy composites via Li substitution

D.B. Deutz,<sup>\*,†</sup> N.T. Mascarenhas,<sup>†</sup> S. van der Zwaag,<sup>†</sup> and W.A. Groen<sup>†,‡</sup>

<sup>†</sup>Novel Aerospace Materials Group, Faculty of Aerospace Engineering, Delft University of Technology, Kluyverweg 1, 2629HS Delft, the Netherlands

<sup>‡</sup>Holst Centre, TNO, High Tech Campus 31, 5605KN Eindhoven, the Netherlands

E-mail: d.b.deutz@tudelft.nl

## Abstract

In this study the influence of Li substitution on the piezoelectric performance of lead free K<sub>0.5</sub>Na<sub>0.5</sub>NbO<sub>3</sub> (KNN)-epoxy composites is explored. Cuboid KNN piezoceramic particles modified with 0 to 12 mol.% of Li are prepared via a double calcination technique. The KNN-based particles are dispersed at 10 vol.% in an epoxy matrix to develop both random and dielectrophoretically structured composites. While the dielectric constant of these composites appears almost independent of Li content, the piezoelectric charge constant of structured composites peaks before the polymorphic phase transition, at 3 mol.% of Li. The enhanced energy harvesting capabilities of these composites make them an interesting choice for flexible energy generators.

# 1 Introduction

Research into flexible piezoelectric materials is on the rise for their potential for strain driven energy harvesting and integration into and onto flexible and wearable electronics.<sup>1,2</sup> Most commercial piezoelectrics are based on ceramics which contain lead atoms in their crystal structure, yet for environmental reasons, lead free materials are preferred.<sup>3,4</sup> Of the lead free ceramics, those based on the morphotropic phase boundary (MPB) composition  $[\text{K}_{0.5}\text{Na}_{0.5}]\text{NbO}_3$  (KNN) doped with Li are a promising candidate for energy harvesting due to their high Curie temperature (around 400 °C), enabling use at a wide range of temperatures, and favorable electrical properties.<sup>3,4</sup> As in many piezoelectric ceramics, compositions near the phase transition at  $[\text{K}_{0.5}\text{Na}_{0.5}]_{(0.94)}\text{Li}_{0.06}\text{NbO}_3$  (KLN6) lead to the best piezoelectric properties.<sup>4-7</sup>

The influence of Li substitution on the piezoelectric and dielectric properties of KNN based ceramics has been investigated extensively.<sup>4-11</sup> In monolithic ceramics Li substitution increases the grain size and the Curie temperature,  $T_C$  [°C], while simultaneously lowering the orthorhombic to tetragonal transition temperature  $T_{O-T}$  [°C].<sup>4-7</sup> A wide range of electrical and mechanical properties have been reported for KNN ceramics doped with Li.<sup>4-11</sup> Despite favorable piezoelectric performance, KNN based ceramics are plagued by variations in the volatilization and segregation of the alkali elements inducing compositional inhomogeneity<sup>8</sup> and the formation of a secondary tetragonal tungsten bronze (TTB) phase<sup>9</sup>, resulting in abnormal grain growth (AGG).<sup>10</sup>

Minor adjustments to the processing scheme change the behavior of the alkali elements and contribute to the ultimate performance of the sintered ceramic.<sup>4,8</sup> Due to the cuboid morphology of the grains KNN based ceramics are notoriously difficult to sinter into dense ceramics. Faster heating rates<sup>9</sup>, inert atmospheres<sup>11</sup>, and long isothermal holds<sup>10</sup> have been reported to inhibit the formulation of strongly faceted cuboid grains, aiding densification.

A number of flexible lead free piezoelectric materials based on a composite of KNN based particles randomly dispersed in a polymer matrix have been developed for piezoelectric energy harvesting.<sup>12-18</sup> The chosen KNN fillers are identical to the compositions developed for optimal properties in ceramics, doped with sintering aids, at or near a polymorphic phase transition (PPT) or MPB. Additionally, these piezoelectric composites require a relatively high volume content of ceramic filler (from 30 vol.% for nanowires up to 85 vol.% for particles) to attain sufficient performance. Besides the volume fraction of filler, piezoelectric performance in electroceramic-polymer composites is affected by: (i) the electrical properties of the filler and matrix, (ii) the size and morphology of the filler, and (iii) the spatial distribution of the filler.<sup>19-22</sup> In KNN based ceramics (i) and (ii) are not independent variables, and altering one (via compositional substitution or processing conditions) will necessarily affect the other.<sup>4-11</sup> The spatial distribution can be controlled by choosing an appropriate composite processing scheme, like dielectrophoretic structurization.<sup>23,24</sup> Applying a dielectrophoretic alignment field on lead based piezoelectric fillers inside an uncured polymer matrix leads to a significant improvement of the piezoelectric performance in composites containing only 10 vol.% of filler compared to randomly dispersed composites.<sup>25</sup> Switching to lead free KNLN6

further improves the performance of structured composites, due to the inherent electrical properties of the filler and the cuboid nature of the particles.<sup>26</sup> However, it is clear from the literature that MPB compositions do not always lead to the best performance in piezoelectric composites.<sup>21,24,27</sup>

Due to the variance in reported KNN based ceramic properties, it is unclear at which amount of Li substitution in KNN the peak performance in piezoelectric properties of composites can be established. Hence, in the present work we will investigate composites based on near PPT  $[\text{K}_{0.5}\text{Na}_{0.5}]_{(1-x)}\text{Li}_x\text{NbO}_3$  (KNLN) particles specifically prepared for embedding in an epoxy matrix and study the effect Li content has on particle morphology, piezoelectric performance and energy harvesting potential.

## 2 Experimental

Five piezoceramic powders were synthesized via solid state reaction with compositions of  $[\text{K}_{0.5}\text{Na}_{0.5}]_{(1-x)}\text{Li}_x\text{NbO}_3$  ( $x = 0$ ,  $x = 0.03$ ,  $x = 0.06$ ,  $x = 0.09$  and  $x = 0.12$ ). Stoichiometric proportions of the >99% pure oxides  $\text{NaCO}_3$ ,  $\text{K}_2\text{CO}_3$ ,  $\text{Li}_2\text{CO}_3$ , and  $\text{Nb}_2\text{O}_5$  (obtained from Sigma Aldrich) were immersed in cyclohexane and milled in glass jars with 5 mm yttria-stabilized ZrO balls. A two step calcination scheme was employed to obtain cuboid particles.<sup>26</sup> Each KNLN powder was calcined at 1050 °C for 3 hours (heated with a rate of 5 °C/min), milled for 5 hours, and calcined again at 950 °C for 20 hours (heated with a rate of 1 °C/min). To break apart loose aggregates, the calcined powders were ultrasonicated for 1 hour and sieved through a 63 µm mesh. All KNLN powders were dried overnight at 150 °C, and stored under vacuum at room temperature

before processing into composites.

Composite disks were prepared by mixing the KNLN powders in Epotek epoxy 302-3M (Epoxy Technology Inc., Billerica (MA), USA) with a particle volume of 10 %. This optically clear epoxy has been extensively studied as a matrix for dielectrophoretically structured composites<sup>24-26</sup>, and has a relatively high dielectric constant,  $\epsilon_{33}$  [-], of 5.3 at room temperature. The theoretical density of each KNLN powder, calculated from the mass of the unit cell over the unit cell volume, was used to calculate the appropriate mixing ratio for each composite. The KNLN particles were mixed with diglycidyl ether of bisphenol-A (DGEBA) resin for 5 min at 2500 rpm in a SpeedMixer (Hauschild, DAC 150 FVZ, Hamm, Germany). Then the multi-functional aliphatic amine hardener poly(oxypropyl)-diamine (POPD) was added to the KNLN-resin mixture and mixed again for 5 min at 2500 rpm. The uncured composite was degassed in a vacuum for 10 min, mixed for 5 min at 2500 rpm to ensure homogeneous distribution of the particles, and poured into a prepared Teflon mould with circular 14 mm diameter cutouts. Al foil sheets of 50  $\mu\text{m}$  thickness were applied on either side of the mould to act as the electrodes for dielectrophoresis (DEP). Flat samples were formed by clamping the mould between two steel plates. To induce dielectrophoretic structuring an electric field of 1  $\text{kV mm}^{-1}$  was applied at an optimal frequency, ranging from 600 Hz to 1.2 kHz, using a function generator (Agilent, 33210A, Santa Clara (CA), USA) in tandem with a high voltage amplifier (TREK, Model 609E-6, Lockport (NY), USA) at room temperature. The leakage current, peak to peak voltage and phase angle of the DEP field were monitored with an oscilloscope (Tektronix Inc., DSOX2002A, Berkshire, UK). After 1 hour at room temperature the composites were cured on a hot plate (IKA, C-

MAG HS7, Staufen, Germany) at 50 °C in 3 hours, keeping the DEP field applied. Random composites were prepared analogously, without application of an electric field. Next, the composites were ejected from the mould and polished to ensure good contact with electrodes. After post-curing at 120 °C for 1 hour, gold electrodes were applied on either side with a sputter coater (Balzers Union, SCD 040, Liechtenstein). The samples were poled in a rapeseed oil bath (Julabo, SE Class III, 12876, Seelbach, Germany) at 80 °C and 11 kV mm<sup>-1</sup> for 30 min with a DC high voltage amplifier (Heinzinger, PNC 30000, Rosenheim, Germany) and cooled to room temperature while still applying the electric field. The composite samples were aged for at least 24 hours before piezoelectric and dielectric measurements took place.

X-ray diffraction (XRD) (Bruker D8 Advance X-ray diffractometer, Bruker AXS Inc., Karlsruhe, Germany, using Co-K $\alpha$  with EVA software) was used to analyze the crystal structure. UnitCell<sup>28</sup> was used to calculate the lattice parameters from the identified peaks. Particle morphology and spatial distribution of the KNLN particles in the random and structured composites were recorded with a field-emission scanning electron microscope (SEM) (JEOL, JSM-7500F, Nieuw Venne, the Netherlands). Particle size was measured in aqueous solution via laser diffraction (Beckman Coulter LS230, Beckman Coulter Nederland B.V., Woerden, the Netherlands) and from SEM. The piezoelectric charge constant,  $d_{33}$  [pC/N], of the composites was measured with a PM300 Berlincourt type piezometer (Piezotest, London, United Kingdom). The capacitance,  $C$  [pF], and dielectric loss,  $\tan \delta$  [-], were measured at 1 kHz and 1 V with an LCR (Agilent, 4263B, Santa Clara (CA), USA). The  $\epsilon_{33}^T$  was derived from the capacitance. Thickness mode electromechanical coupling coefficients,  $k_t$  [%], and

mechanical quality factors,  $Q_m$  [-], were determined by the IEEE resonance method using an impedance analyzer (Agilent, HP4194A, Santa Clara (CA), USA).

## 3 Results

### 3.1 Structural characterization

The X-ray diffraction patterns of the double calcined KNLN powders are presented in Figure 1, normalized to the highest intensity peak. A single phase orthorhombic perovskite phase was observed in the undoped KNN and 3 mol.% Li specimens. Increasing the amount of Li beyond 3 mol.% results in the development of a minor secondary phase, indexed as  $K_3Li_2Nb_5O_{15}$  (ICDD:52-0157) with a non-perovskite tetragonal tungsten bronze (TTB) structure. The development of the TTB phase has been attributed to the volatilization (of K) and segregation (of Na and Li) of the alkali elements during the prolonged post calcination.<sup>7,10,29</sup> At 6 mol.% Li, a coexistence of a tetragonal and orthorhombic phase could be expected, but the specimen tends towards an orthorhombic crystal structure presumably due to loss of Li to the TTB phase. The KNN specimens doped with 9 and 12 mol.% of Li display a tetragonal crystal structure. Figure 1b shows a magnification of the  $2\theta$  range running from  $36^\circ$  to  $39^\circ$ , where the inversion in peak splitting due to Li can be clearly seen.

### 3.2 Particle morphology

Double calcination of the KNLN particulate with 20 h of annealing at  $950^\circ\text{C}$ , by slowly heating at  $1^\circ\text{C}/\text{min}$ , has lead to the formation of cuboid particles (Figure 2). Small



cuboid particles on the order of 0.5 to 1.0  $\mu\text{m}$  with strongly faceted edges have developed in the undoped KNN. Doping with Li increases the size of the cuboid particles. At 6 mol.% of Li the particle size decreases slightly, and some columnar shaped particles, likely TTB phase, on the order of 0.5  $\mu\text{m}$  are observed. At 9 and 12 mol.% the cuboid particles develop serrated, roughened edges around faceted surfaces, and many of the particles have fractured. It is difficult to distinguish whether the clusters of cuboid grains have sintered together to form aggregates or are free flowing from SEM alone. Therefore, the particle size was measured in aqueous solution via laser diffraction. However, since the particles tend to agglomerate, the particle dispersion was not representative of the actual particle size distribution.

### 3.3 Composite microstructure

In Figure 3 the cross-section of the composite microstructures of the KNLN particulates processed into both random and structured composites at 10 vol.% of filler are shown. It is immediately clear that the double calcination of the KNLN particulates has led to aggregation of particles. Even so, the dispersion of the primary particles and aggregates is relatively homogeneous in both random and structured composites. Comparing the microstructure of random composites to structured, it is clear that the application of the dielectrophoretic structuring field has induced the KNLN particles to align into chains parallel to the direction of the electric field. Chains of primary particles are interspersed with large aggregates. Compositions with a larger relative volume of primary particles (the undoped KNN and 12 mol.% of Li) more clearly show the formation of chain like structures in the direction of the applied electric field, compared to their random

counterparts.

### 3.4 Dielectric properties

The variation of the dielectric constant and dielectric loss of the KNLN-epoxy composites is shown in Figure 4 as a function of Li content. In structured composites, the dielectric constant trends upward with Li. Any variation in dielectric properties or morphology of the particles has no effect on the dielectric constant in random composites, which remains at a flat constant around 8.5. The dielectric loss of the composites is below 5 %, and the trends with respect to Li content are in line with the dielectric constant. Structuring of the KNLN particles has marginally increased the dielectric constant and loss over all Li contents. The dielectric loss remains unchanged after 1 year stored at ambient conditions, indicating that encapsulation of the KNLN particles in the composites appears to inhibit the moisture absorption commonly reported for Li-doped KNN ceramics.

### 3.5 Piezoelectric properties

The influence of Li content on the piezoelectric charge constant of 10 vol.% KNLN-epoxy composites is presented in Figure 5. The piezoelectric charge constant is dependent on the phase structure, and higher on the orthorhombic side. In random composites this translates to a relative constant of 5 pC/N on the orthorhombic side, and 2 pC/N for the tetragonal compositions. The properties are improved by dielectrophoretic structuring of the KNLN particles, and a peak in piezoelectric charge constant can be

identified at 3 mol.% of Li with 19.4 pC/N.

In application as a sensor or an off-resonance energy harvester, the piezoelectric voltage constant,  $g_{33}$  [mV.m/N], and figure of merit,  $d_{33} \cdot g_{33}$  [pm<sup>3</sup>/J], of the KNLN-epoxy composites are of the utmost importance. The  $g_{33}$  is calculated via:  $g_{33} = d_{33}/(\epsilon_{33}^T \cdot \epsilon_0)$ , where  $\epsilon_0$  is the permittivity of free space and the  $\epsilon_{33}^T$  is measured at 110 Hz. These figures are presented as a function of Li content in Figure 6. The maximum values obtained in random composites are 68 mV.m/N and 0.43 pm<sup>3</sup>/J with undoped KNN, while for structured composites the maximum attained values are 181 mV.m/N and 3.5 pm<sup>3</sup>/J, at 3 mol.% Li. The magnitude and position of the maximum  $g_{33}$  value in structured composites depends on the stiffness ratio of the piezoelectric phase over the polymer phase, and it is likely that higher values could be obtained at lower particle volume fractions, while increases in  $d_{33} \cdot g_{33}$  could be expected at slightly higher volume fractions.<sup>25,26</sup>

The piezoelectric performance of the structured orthorhombic KNLN composites could also be studied via frequency response analysis, due to the relatively high attained  $d_{33}$  (Figure 5). The materials properties are summarized in Table 1, where each value is the average of three samples per Li content, with dimensions of 9 mm in diameter and approximately 1 mm thickness. The mechanical loss factor,  $\Phi$ , is evaluated from the resonance peak in the frequency dependence of the real part of the impedance,  $Z'$ , via  $\Phi = (f_1 - f_2)/f_{peak}$ , where  $f_1$  and  $f_2$  are the frequencies at which the impedance is equal to  $Z'_{peak}/\sqrt{2}$ . The mechanical quality factors follow from the relation  $Q_m = 1/\Phi$ . The  $k_t$  was evaluated from the following equation, where  $f_s$  and  $f_p$  are the series and parallel

resonance frequencies.<sup>30</sup>

$$k_t = \frac{\pi f_s}{2 f_p} \tan\left(\frac{\pi \Delta f}{2 f_p}\right) \quad (1)$$

For materials with high mechanical losses, the IEEE recommends approximating  $\Delta f$  from the following equations, directly from the minimum,  $f_m$ , and maximum resonance frequencies,  $f_n$ , via a figure of merit ' $M$ '.<sup>30,31</sup>

$$\Delta f = (f_p - f_s) \approx \frac{f_n - f_m}{\sqrt{1 + \frac{4}{M^2}}} \quad (2)$$

$$M = \frac{1}{2\pi f_s R_1 C_0} \approx \frac{1}{2\pi f_m (C_0 + C_1) |Z_m|} \quad (3)$$

The sum of  $C_0$  and  $C_1$  (representing the capacitance of the parallel and series branch of the equivalent circuit of the piezoelectric material near resonance) is equivalent to the static capacitance measured below the fundamental resonance, at 1 kHz.  $R_1$  is the resistance of the series branch of the equivalent circuit and  $|Z_m|$  is the impedance minimum at resonance. Finally, the frequency constant,  $N_t^D$  [Hz.m], was calculated from  $N_t^D = f_p \cdot t$ , where  $t$  [mm] is the sample thickness, leading to the longitudinal velocity  $C_l$  [m/s] equal to  $2N_t^D$ .

## 4 Discussion

From the above results we can propose the following processes take place in the studied electroceramic-polymer composites. Substituting Li in MPB cuboid KNN particles increases the particle size, but leads to the formation of a secondary non-perovskite phase. The presence of the TTB phase in the KNLN composites with 6 to 12 mol.% of Li lowers the effective amount of polarizable volume, decreasing performance in composites. At 3 mol.% of Li no such TTB phase is discernible from XRD. While the coarsening and necking between the particles at 9 and 12 mol.% of Li is considered to be related to the well studied lower temperature of the liquid phase formation in these compositions<sup>4,7</sup>, the decrease in particle size at 6 mol.% of Li would indicate a change in the particle formation mechanism. The observed fracturing of the high Li content particles may be attributed to the high degree of tetragonality leading to high strains during cooling, and could signal a secondary mechanism of decreased performance in composites. In the particle size range observed from SEM (from 1.0  $\mu\text{m}$  in the undoped KNN to  $>5$  at 9 and 12 mol.% Li) we would expect to see a dependency of the  $d_{33}$  of random composites on particle size.<sup>21,22</sup> The absolute value of the  $d_{33}$  is also higher than one would expect at 10 vol.% of filler from existing models for monodisperse particles in a dilute medium.<sup>20</sup> This suggests that the observed aggregates dominate the performance in random composites, regardless of the variance in electrical properties of the filler as a function of Li content. Structuring the KNLN particles in an epoxy matrix has enhanced the  $d_{33}$  and  $\varepsilon'_{33}$  with respect to random composites, and previous work at the PPT<sup>26</sup>, showing that dielectrophoretic structurization is a robust method of improving

piezoelectric performance in composites. Figure 4 suggests that the dielectric constant increases with Li content, except at 6 mol.% where the particle size decreases slightly. Since larger particles lead to fewer polymer interfaces per aligned chain<sup>23</sup>, we suggest the increase in dielectric constant is a particle size effect. Similar to random composites, the  $d_{33}$  of the structured orthorhombic composites outperforms tetragonal compositions. Yet there is a peak at 3 mol.% of Li, not evident from the results of random composites. In structured electroceramic-polymer composites the morphology and size of the particles will affect the efficiency of chain formation due to dielectrophoresis and degree of poling.<sup>24,25,32</sup> And it has been demonstrated that particle size distribution is a key factor in the chain formation of structured composites.<sup>33</sup> The significant decrease in polymer interfaces in structured composites allows the inherent electrical properties of the filler to somewhat overcome the aggregate dominated behavior observed in random composites. Even though the piezoelectric charge constant of the particles at 6 mol.% Li outperforms 3 mol.% Li, the reduction in polymer interfaces due to the larger particle size results in a better performance at 3 mol.% in composites. Furthermore, since the aim of the work is to enhance energy harvesting potential, the reduction in the dielectric constant, in the 3 mol.% Li composites after poling can compensate for the inherently lower  $d_{33}$  of the composition.<sup>5</sup> The peak in performance observed at 3 mol.% of Li can then be attributed to the increase in primary particle size, supplemented by aggregates which enhance overall performance via reduced inter-particle distance. To examine the energy harvesting potential of the KNLN based composites, a comparison of the piezoelectric performance of the composites from this study is drawn with piezoelectric materials from the literature in Table 2. The piezoelectric composites are ranked according to the volume

fraction of active material. To attain a  $d_{33}$ ,  $k_t$ , and figure of merit similar to what we have demonstrated for 10 vol.% structured KNLN3-epoxy in random composites, a combination of high volume fractions of active material, large particle sizes and high dielectric constant polymer matrices are necessary.<sup>22,34-36</sup> In lead free composites based on KNN, similar properties have only been reported for 1-3 composites, or volume contents of active material over 0.7.<sup>15-17</sup> While the figure of merit of the KNLN3 composite approaches that of the KNN bulk ceramic, an order of magnitude lower than PZT ceramics, the performance is similar to pure PVDF and its copolymers at significantly reduced dielectric loss.

## 5 Conclusions

This work demonstrates that a significant improvement of the piezoelectric properties of electroceramic polymer composites can be achieved by dielectrophoretic alignment of KNLN particles with a wide distribution in particle size over lead containing composites. A peak in performance of structured composites was identified in KNN doped with 3 mol.% of Li, a single phase orthorhombic composition with cuboid particle morphology. There are indications that it is the combination of favorable electrical properties and particle morphology at  $[\text{K}_{0.5}\text{Na}_{0.5}]_{(0.97)}\text{Li}_{0.03}\text{NbO}_3$  leading to the peak in piezoelectric performance. Compared to 0 and 6 mol.% larger particle sizes have been attained, lowering the amount of polymer interfaces per chain. Although a lower homogeneity of the composite microstructure is attained, the performance at 10 vol.% is now such that the electromechanical coupling can be measured via frequency response analysis. Due to

the enhanced piezoelectric energy harvesting figure of merit,  $d_{33}g_{33}$ , composites based on these materials are an interesting choice for flexible energy generators and within the competitive realm of PVDF and its copolymers.

## Acknowledgement

This work was made possible thanks to a research grant from the European Commission, FP7 NMP program, under grant no. 310311.

## References

- [1] J. Rödel, K. G. Webber, R. Dittmer, W. Jo, M. Kimura, and D. Damjanovic, "Transferring lead-free piezoelectric ceramics into application," *Journal of the European Ceramic Society* **35**(6), 1659-1681 (2015).
- [2] C. R. Bowen, H. A. Kim, P. M. Weaver, and S. Dunn, "Piezoelectric and ferroelectric materials and structures for energy harvesting applications," *Energy & Environmental Science*, **7**, 25-44 (2014).
- [3] T. R. Shrout and S. J. Zhang, "Lead-free piezoelectric ceramics: Alternatives for PZT? *Journal of Electroceramics*" **19**(1), 113-126 (2007).
- [4] J.-F. Li, K. Wang, F.-Y. Zhu, L.-Q. Cheng, and F.-Z. Yao, "(K,Na)NbO<sub>3</sub>-based lead-free piezoceramics: Fundamental aspects, processing technologies, and remaining challenges," *Journal of the American Ceramic Society* **96**(12), 3677-3696 (2013).
- [5] Y. Saito, H. Takao, T. Tani, T. Nonoyama, K. Takatori, *et al.*, "Lead-free piezoceramics," *Nature* **432**, 84-87 (2004).
- [6] Y. Guo, K.-i. Kakimoto, and H. Ohsato, "Phase transitional behavior and piezoelectric properties of (Na<sub>0.5</sub>K<sub>0.5</sub>)NbO<sub>3</sub>-LiNbO<sub>3</sub> ceramics," *Applied Physics Letters* **85**(18), 4121 (2004).
- [7] M. Matsubara, T. Yamaguchi, K. Kikuta, and S.-I. Hirano, "Effect of Li substitution on the piezoelectric properties of potassium sodium niobate ceramics," *Japanese Journal of Applied Physics* **44**(8), 6136-6142 (2005).
- [8] Y. Wang, D. Damjanovic, N. Klein, E. Hollenstein, and N. Setter, "Compositional inhomogeneity in Li- and Ta-modified (K,Na)NbO<sub>3</sub> ceramics," *Journal of the American*



*Ceramic Society* **90**(11), 3485-3489 (2007).

[9] D. Liu, H. Du, F. Tang, F. Luo, D. Zhu, *et al.*, "Effect of heating rate on the structure evolution of  $(K_{0.5}Na_{0.5})NbO_3$ - $LiNbO_3$  lead-free piezoelectric ceramics," *Journal of Electroceramics* **20**(2), 107-111 (2007).

[10] Y. Wang, D. Damjanovic, N. Klein, and N. Setter, "High-temperature instability of Li- and Ta-Modified  $(K,Na)NbO_3$  piezoceramics," *Journal of the American Ceramic Society* **91**(6), 1962-1970 (2008).

[11] X. Vendrell, J. García, F. Rubio-Marcos, D. Ochoa, L. Mestres, *et al.*, "Exploring different sintering atmospheres to reduce nonlinear response of modified KNN piezoceramics," *Journal of the European Ceramic Society* **33**(4), 825-831 (2013).

[12] C. K. Jeong, K.-I. Park, J. Ryu, G.-T. Hwang, and K. J. Lee, "Large-area and flexible lead-free nanocomposite generator using alkaline niobate particles and metal nanorod filler," *Advanced Functional Materials* **24**, 2620-2629 (2014).

[13] M. K. Gupta, S.-W. Kim, and B. Kumar, "Flexible high-performance lead-free  $Na_{0.47}K_{0.47}Li_{0.06}NbO_3$  microcube-structure-based piezoelectric energy harvester," *ACS Applied Materials & Interfaces* **8**, 1766-1773 (2016).

[14] Q.-t. Xue, Z. Wang, H. Tian, Y. Huan, Q.-Y. Xie, *et al.*, "A record flexible piezoelectric KNN ultrafine-grained nanopowder-based nanogenerator," *AIP Advances* **5**(1), 017102 (2015).

[15] J.-H. Seol, J. S. Lee, H.-N. Ji, Y.-P. Ok, G. P. Kong, *et al.* "Piezoelectric and dielectric properties of  $(K_{0.44}Na_{0.52}Li_{0.04})(Nb_{0.86}Ta_{0.10}Sb_{0.04})O_3$ -PVDF composites," *Ceramics International* **38**, S263-S266 (2012).

[16] D. T. Le, N. B. Do, D. U. Kim, I. Hong, I.-W. Kim, *et al.*, "Preparation and characterization of lead-free  $(K_{0.47}Na_{0.51}Li_{0.02})(Nb_{0.8}Ta_{0.2})O_3$  piezoceramic/epoxy composites with 0-3 connectivity," *Ceramics International* **38**, S259-S262 (2012).

[17] Z.-Y. Shen, J.-F. Li, R. Chen, Q. Zhou, and K. K. Shung, "Microscale 1-3-type  $(Na,K)NbO_3$ -based Pb-free piezocomposites for high-frequency ultrasonic transducer applications," *Journal of the American Ceramic Society* **94**(5), 1346-1349 (2011).

[18] Y. Yang, J. H. Jung, B. K. Yun, F. Zhang, K. C. Pradel, *et al.*, "Flexible pyroelectric nanogenerators using a composite structure of lead-free  $KNbO_3$  nanowires," *Advanced Materials* **24**(39), 5357-5367 (2012).

[19] R. E. Newnham, D. P. Skinner, and L. E. Cross, "Connectivity and piezoelectric-pyroelectric composites," *Materials Research* **13**, 525-536 (1978).

[20] T. Yamada, T. Ueda, and T. Kitayama, "Piezoelectricity of a high-content lead zirconate titanate/polymer composite," *Journal of Applied Physics* **53**(6), 4328-4332 (1982).

- [21] D. M. Reed, T. T. Srinivasan, Q. C. Xu, and R. E. Newnham, "Effect of particle size on the dielectric and piezoelectric properties of  $\text{PbTiO}_3$ -polymer composites," in *IEEE 7th International Symposium on Applications of Ferroelectrics*, 324–327 (1990).
- [22] K. Han, A. Safari, and R. E. Riman, "Colloidal processing for improved piezoelectric properties of flexible 0-3 ceramic-polymer composites," *Journal of the American Ceramic Society* **74**(7), 1699-1702 (1991).
- [23] C. P. Bowen, R. E. Newnham, and C. A. Randall, "Dielectric properties of dielectrophoretically assembled particulate-polymer composites," *Journal of Materials Research* **13**(1), 205-210 (1998).
- [24] S. A. Wilson, G. M. Maistros, and R. W. Whatmore, "Structure modification of 0-3 piezoelectric ceramic/polymer composites through dielectrophoresis," *Journal of Applied Physics D: Applied Physics* **38**(2), 175-182 (2005).
- [25] D. A. van den Ende, B. F. Bory, W. A. Groen, and S. van der Zwaag, "Improving the  $d_{33}$  and  $g_{33}$  properties of 0-3 piezoelectric composites by dielectrophoresis," *Journal of Applied Physics* **107**, 024107 (2010).
- [26] N. K. James, D. B. Deutz, R. K. Bose, S. van der Zwaag, and P. Groen, "High piezoelectric voltage coefficient in structured lead-free  $(\text{K},\text{Na},\text{Li})\text{NbO}_3$  particulate-epoxy composites," *Journal of the American Ceramic Society JACERS-38016.R1*, In press (2016).
- [27] A. S. Karapuzha, N. K. James, S. van der Zwaag, and W. A. Groen, "On the use of non- MPB lead zirconium titanate (PZT) granules for piezoelectric ceramic-polymer sensorial composites," *Journal of Materials Science: Materials in Electronics* **27**(9), 9683–9689 (2016).
- [28] T. Holland and S. Redfern, "Unit cell refinement from powder diffraction data: the use of regression diagnostics," *Mineralogical Magazine* **61**(1), 65-77 (1997).
- [29] K. Wang, J.-F. Li, and N. Liu, "Piezoelectric properties of low-temperature sintered Li-modified  $(\text{Na},\text{K})\text{NbO}_3$  lead-free ceramics," *Applied Physics Letters* **93**, 092904 (2008).
- [30] A. Meitzler, D. Berlincourt, G. Coquin, F. Welsh, H. Tiersten, *et al.*, "IEEE Standards on piezoelectricity", New York: The Institute of Electrical and Electronics Engineers, (1987).
- [31] T. Gururaja, W. Schulze, L. Cross, R. Newnham, B. Auld, *et al.*, "Piezoelectric composite materials for ultrasonic transducer applications. Part I: Resonant rod-polymer composites," *IEEE Transactions on Sonics and Ultrasonics* **SU-32**(4), 481-498 (1985).
- [32] T. B. Jones, *Electromechanics of particles*. Cambridge University Press (1995).
- [33] M. Gutiérrez, H. Khanbareh, and S. van der Zwaag, "Computational modeling of

structure formation during dielectrophoresis in particulate composites,” *Computational Materials Science* **112**, 139-146 (2016).

[34] A. Pelaiz-Barranco and P. Marin-Franch, “Piezo-, pyro-, ferro-, and dielectric properties of ceramic/polymer composites obtained from two modifications of lead titanate,” *Journal of Applied Physics* **97**(3), 034104 (2005).

[35] L. Pardo, J. Mendiola, and C. Alemany, “Theoretical treatment of ferroelectric composites using Monte Carlo calculations,” *Journal of Applied Physics* **64**(10), 5092 (1988).

[36] C. J. Dias and D. K. Das-Gupta, “Inorganic ceramic/polymer ferroelectric composite electrets,” *IEEE Transactions on Dielectrics and Electrical Insulation* **3**(5), 706-734 (1996).

[37] E. A. Dijkstra, “Ultrasonic distance detection in spinal cord stimulation,” Ph.D.thesis, University of Twente (2003).

[38] “Morgan Advanced Materials Technical Datasheet PZT500 Series,” (2013).

Table 1: Electromechanical properties of 10 vol.% structured orthorhombic KNLN-epoxy composites from the thickness mode resonance.

Li	$M$	$k_t$	$Q_m$	$N_t^D$	$C_t$
[x]	[-]	[%]	[-]	[Hz.m]	[m/s]
0.00	0.93	13.6	21	1211	2422
0.03	0.97	26.8	15	1376	2751
0.06	0.95	15.0	25	1217	2433

Table 2: Performance of reported piezoelectric materials compared to this work.

Active material	Active volume [%]	Matrix	$d_{33}$ [pC/N]	$k_t$ [-]	$\tan \delta_e$ [%]	$d_{33} \cdot g_{33}$ [pm <sup>3</sup> /J]	Ref.
Structured KNLN3	10	Epoxy	19	0.27	2.3	3.52	This work
KNN	10	Epoxy	5		0.9	0.34	This work
Structured PZT5A	10	Epoxy	7			0.52	<sup>25</sup>
Structured KNLN	10	Epoxy	13			1.53	<sup>26</sup>
PTCa	50	PEKK	28	0.17	1.2	3.60	<sup>34</sup>
PZT	57	Epoxy	<sup>1</sup> 140			<sup>1</sup> 6.15	<sup>35</sup>
PTCa	65	PVDF-TrFE	54	0.24		4.83	<sup>36</sup>
PT-BFMn	65	Epoxy	65		3.2		<sup>22</sup>
KNNLST	70	PVDF	33		7.0	14.9	<sup>15</sup>
KNNLT	85	Epoxy	44			1.05	<sup>16</sup>
1-3 Dice and fill NKNL	25	Epoxy	140		4.8	7.33	<sup>17</sup>
PVDF	100	-	16	0.11	24	5.11	<sup>37</sup>
PVDF-TrFE	100	-	15	0.26	11	5.60	<sup>37</sup>
KNN	100	-	127	<sup>2</sup> 0.41	3.6	4.25	<sup>5</sup>
KNNLT	100	-	230		1.6	4.76	<sup>5</sup>
PZT5A4	100	-	460	0.55	1.7		<sup>38</sup>
PZT507	100	-	820	0.40	1.6	12.9	<sup>38</sup>
						17.3	

<sup>1</sup> Average particle size is larger than sample thickness

<sup>2</sup>  $k_t$  from <sup>6</sup>

Figure 1: XRD patterns (a) of  $[K_{0.5}Na_{0.5}]_{(1-x)}Li_xNbO_3$  (KNLN) ( $x = 0$ ,  $x = 0.03$ ,  $x = 0.06$ ,  $x = 0.09$  and  $x = 0.12$ ), and (b) a magnification of the range  $36^\circ$  to  $39^\circ 2\theta$ .

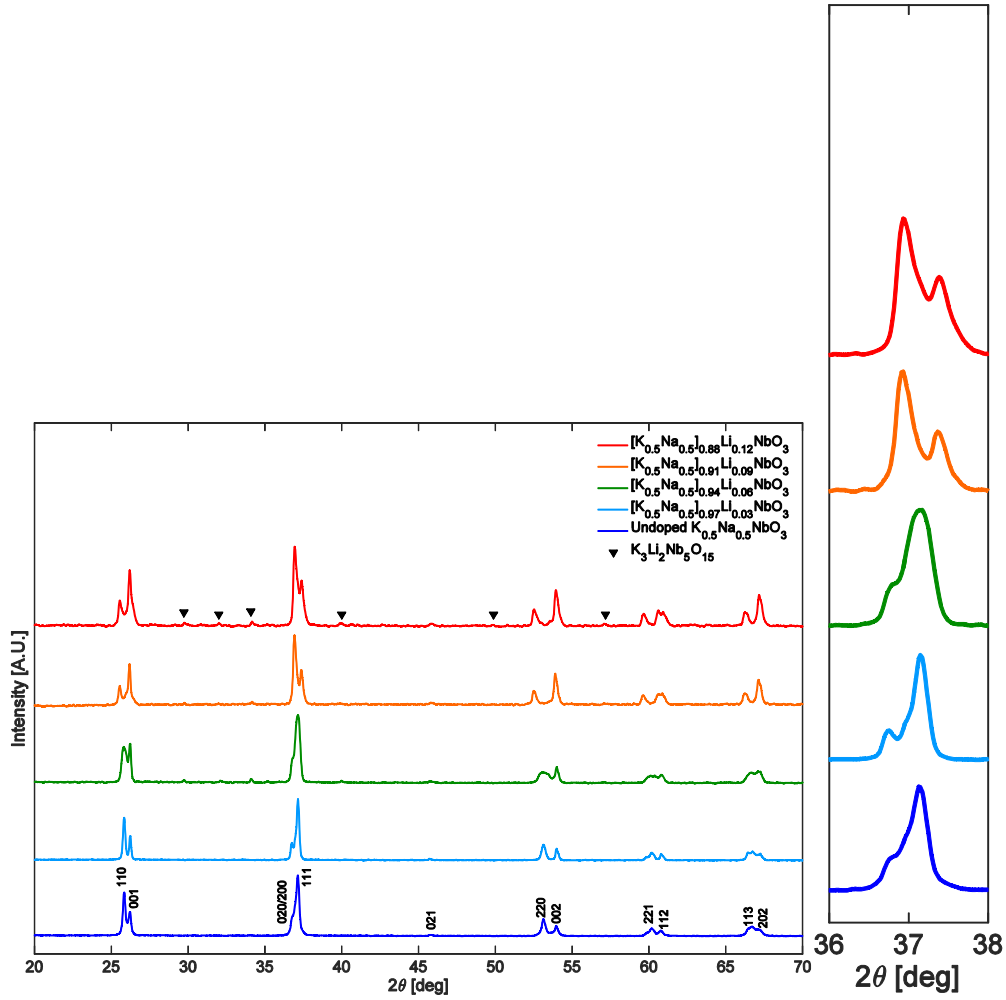


Figure 2: Micrographs of the two-step calcined KNLN particles (at 2000x (left) and 10000x (right) magnification), with increasing Li content: (a) undoped KNN, (b) 3 mol.%, (c) 6 mol.%, (d) 9 mol.% and (e) 12 mol.%.

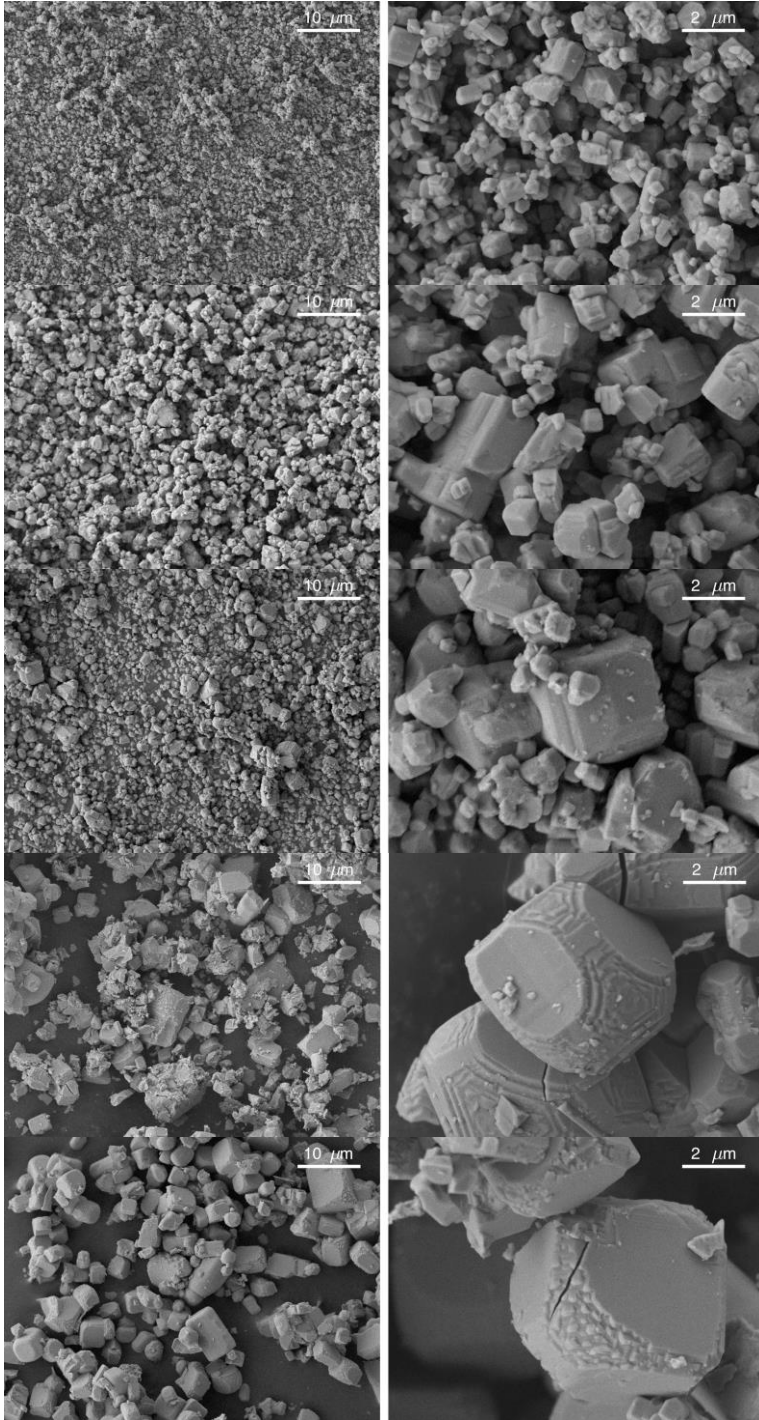


Figure 3: Micrographs of the cross-section of 10 vol.% KNLN-epoxy composites (magnification 200x) with (a) Undoped KNN, (b)  $x = 0.03$ , (c)  $x = 0.06$ , (d)  $x = 0.09$ , (e)  $x = 0.12$ . The 'R' and 'S' stand for random and structured composites, respectively.

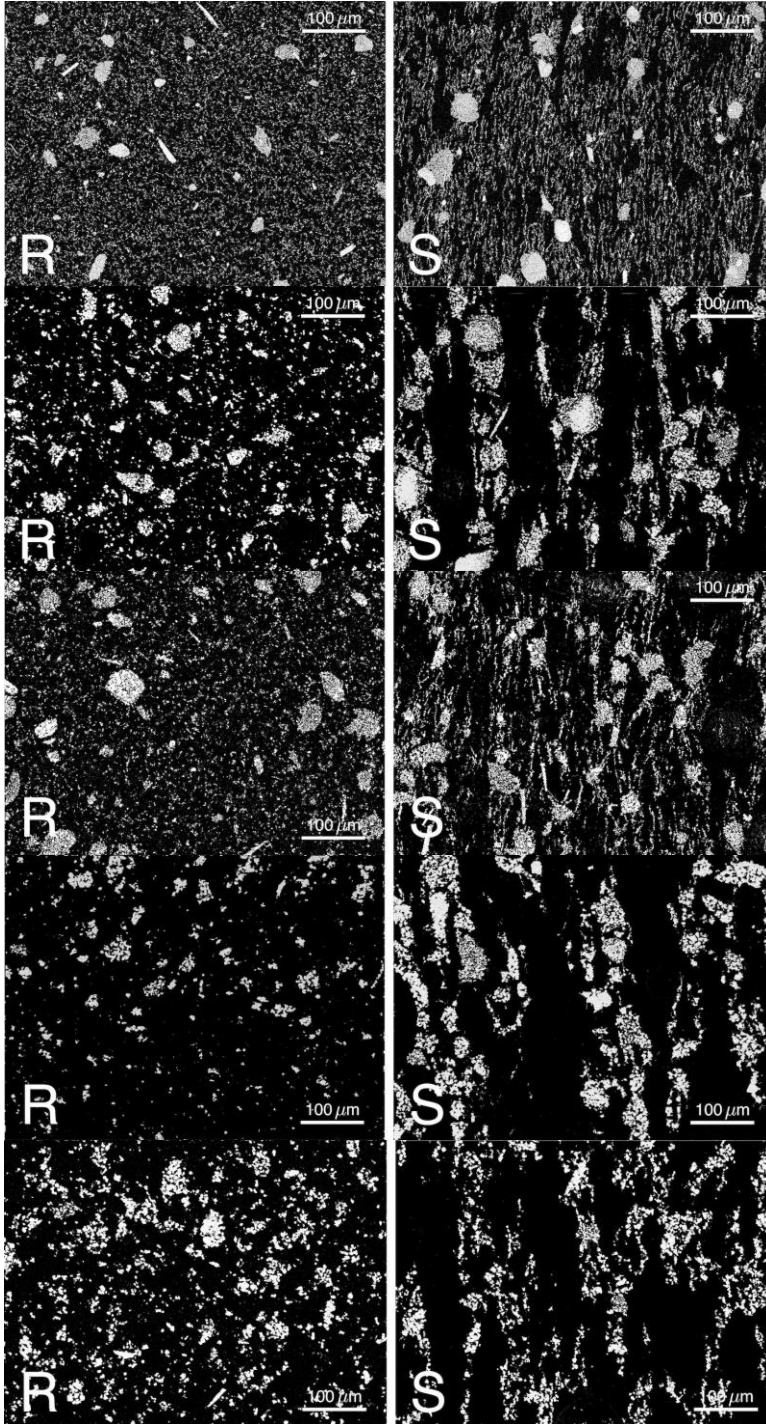




Figure 4: Variation of the dielectric constant (a) and the dielectric loss (b) of random and structured KNLN-epoxy composites due to Li dopant. The lines are a guide for the eye.

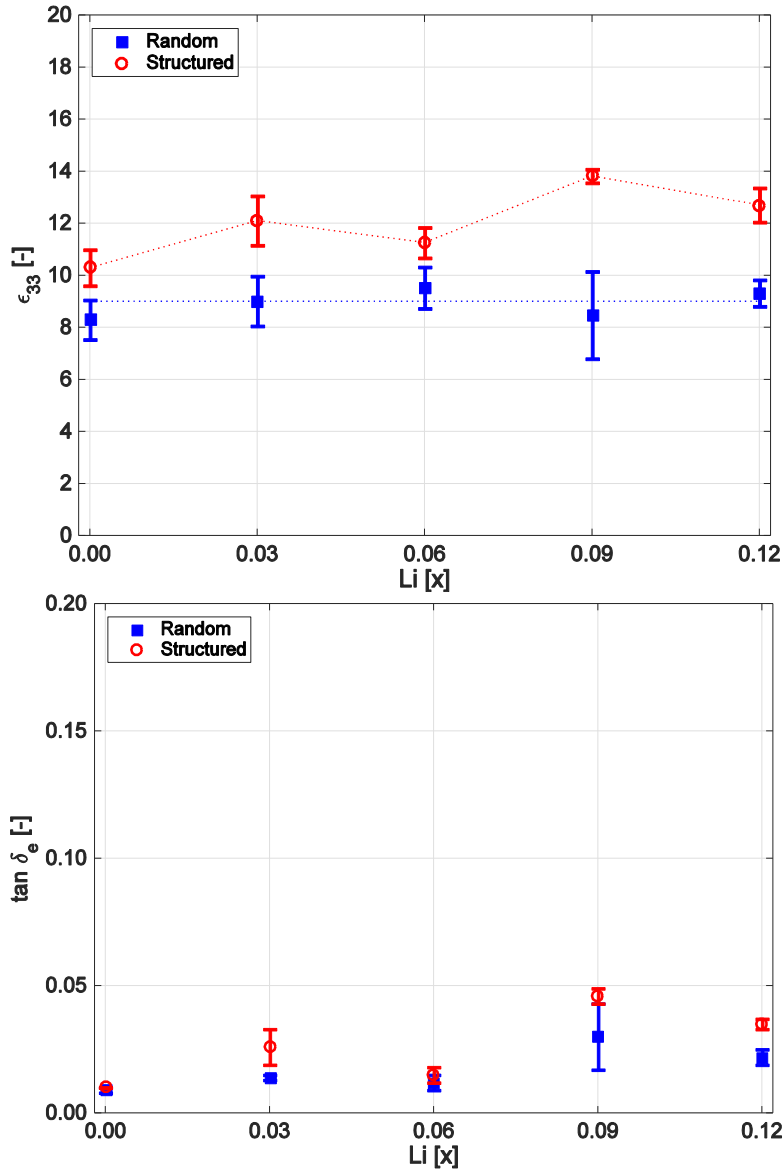


Figure 5: Variation of the piezoelectric charge constant due to Li dopant in random and structured KNLN-epoxy composites. The lines are a guide for the eye.

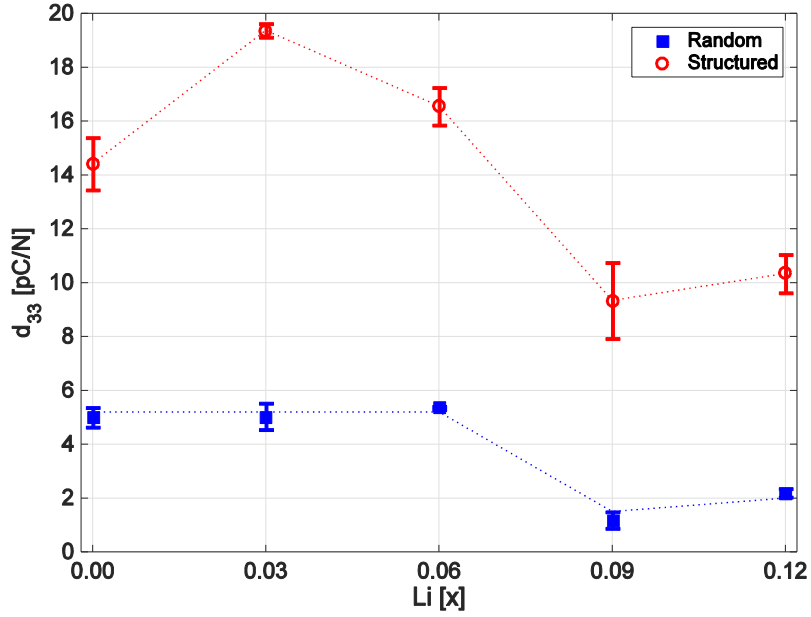
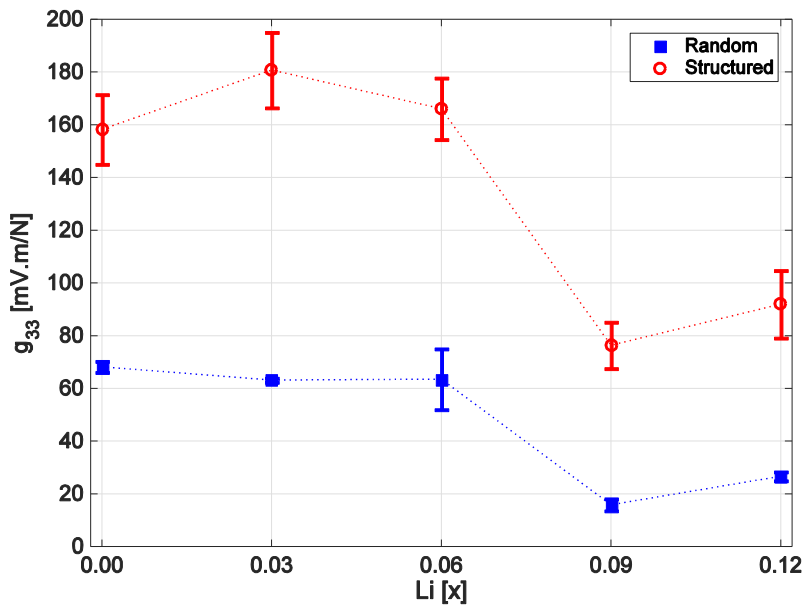


Figure 6: Piezoelectric voltage constant (a) and figure of merit ( $d_{33} \cdot g_{33}$ ) (b) of random and structured 10 vol.% KNLN-epoxy composites versus Li content. The lines are a guide for the eye.



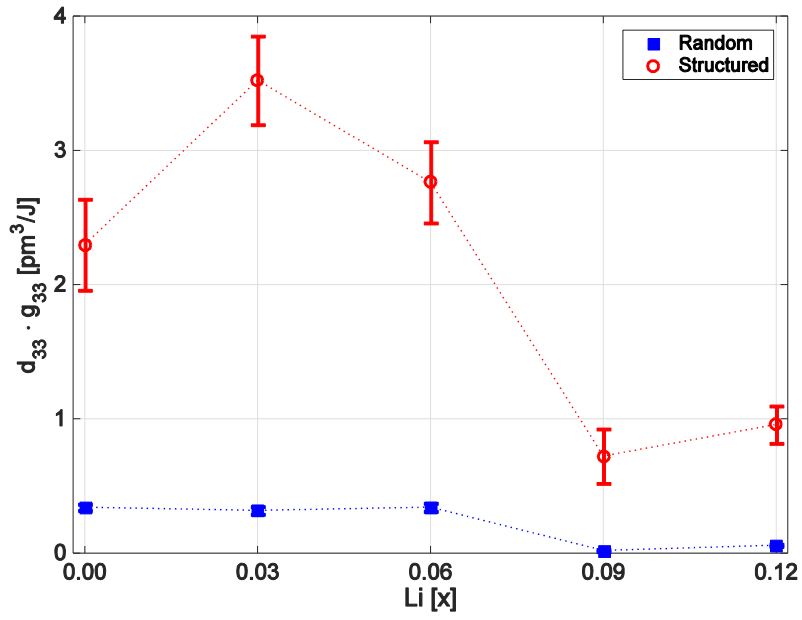


Figure 7: Raw frequency response (phase angle and impedance) of a structured KNLN3-epoxy composite.

